

# A New Compensation Method for Emission Degradation in an AMOLED Display Via an External Algorithm, New Pixel Circuit, and Models of Prior Measurements

Kuei-Yu Lee, Yen-Ping Hsu, Paul C.-P. Chao, *Member, IEEE*, and Wei-Dar Chen

**Abstract**—A new external algorithm with sensing circuit are proposed to compensate AMOLED display degradation. The compensation is enabled by first evaluating degradation level of OLEDs based on the OLED anode voltages detected by a newly-designed sensing subcircuit. According to sensed voltages, the external algorithm selects appropriate built-in models to compensate OLED degradation with the aim to achieve expected OLED emitted luminance. The models are established based on prior measurements to prescribe the relations between luminance and current ( $L - I$ ) and luminance and voltage ( $L - V$ ) of each OLED. In this way of compensation, the proposed method is able to incorporate negative effects of OLED degradation aggravation while increasing driving current to compensate the original decay in OLED luminance. Moreover, another algorithm along with the 4T0.5C pixel circuit as presented in prior studies are adopted to compensate process variation in  $V_{th}$  among pixels for improving the emission uniformity of an AMOLED panel. Experiments are conducted by combining the external algorithm with sensing circuit and the pixel circuit to validate the performances of compensating and alleviating OLED degradation.

**Index Terms**—Active-matrix organic light-emitting diode (AMOLED), aggravated degradation, alleviation, compensation.

## I. INTRODUCTION

ACTIVE-MATRIX organic light-emitting diode (AMOLED) displays are largely considered to be the most popular displays of next generation. These have various merits including high brightness, high efficiency, wide viewing angle, and simple structure [1]. Recently, small-sized AMOLED panels are employed in mobile phones. However, for large-sized AMOLED panels, the troublesome drawbacks like OLED degradation and panel non-uniformity still hinder AMOLED displays to replace LCD TVs in the future.

Manuscript received March 14, 2013; revised July 09, 2013 and October 21, 2013; accepted November 16, 2013. Date of publication November 25, 2013; date of current version February 11, 2014. This work was supported in part by the UST-UCSD International Center of Excellence in Advanced Bio-Engineering sponsored by the Taiwan National Science Council I-RiCE under Grant NSC-101-2911-I-009-101.

The authors are with the Department of Electrical Engineering, National Chiao Tung University, Hsinchu 300, Taiwan (e-mail: pchao@mail.nctu.edu.tw).

Color versions of one or more of the figures are available online at <http://ieeexplore.ieee.org>.

Digital Object Identifier 10.1109/JDT.2013.2292555

As for OLED degradation, some research works were proposed to explore the phenomenon of OLED degradation. The stated causes for degradation are like accumulative holes [2], the impurity of movable ions [3], [4], or the Indium move [5]. All the aboves lead to decay in the organic emitting layer during long-time drives. To remedy the problem, some past works proposed the known means of reverse bias [6], [7] to alleviate degradation of a single emitting OLED chip. Another study was later conducted in [8] to propose the application of reverse bias on a 5T1C pixel circuit with a relatively large layout area of the employed pixel circuit. A new 4T0.5C pixel circuit with reverse bias enabled in a smaller layout area was presented in [9] later to increase OLED panel resolution to a required level. Although the OLED degradation was alleviated successfully on the experiment results in [8], [9], it still needs a detailed, concrete compensation algorithm to ensure OLED emission to expected luminance levels with inevitable OLED degradation present. Chaji *et al.* [10] proposed a method to compensate OLED current to desired value based on sensed current, expecting that the OLED emission luminance is compensated. This method however fails to achieve accurate compensation due to possible degradation in OLED emitted luminance with respect to a given current over a long period of operation. Kohno *et al.* in [11] proposed a pixel circuit to improve image-sticking, but it did not address how to compensate OLED degradation. Lin *et al.* [12] proposed the approaches of current compensation, where the current through an OLED component was adjusted larger to maintain originally-designed emitted luminance. These larger currents, however based on basic operation principles of OLEDs, aggravate OLED degradation, leading to a further change in OLED electro-optical behaviors and thus posing greater difficulty in compensating OLED degradation. On the other hand, In *et al.* [13], [14] and Min *et al.* [15] evaluated the OLED luminance degradation by detecting the voltage across the OLED, and then proposed an external algorithm to compensate the luminance decay. The degradation evaluation is done based on a measured relation between the OLED anode voltage increments and its normalized luminance. However, the relation is most likely not to be precisely preserved for the OLEDs driven in varied levels of currents for an extensive time of compensations, since the OLED would experience significant changes in electro-optical behaviors [3], [4], leading to possible imprecise compensations.

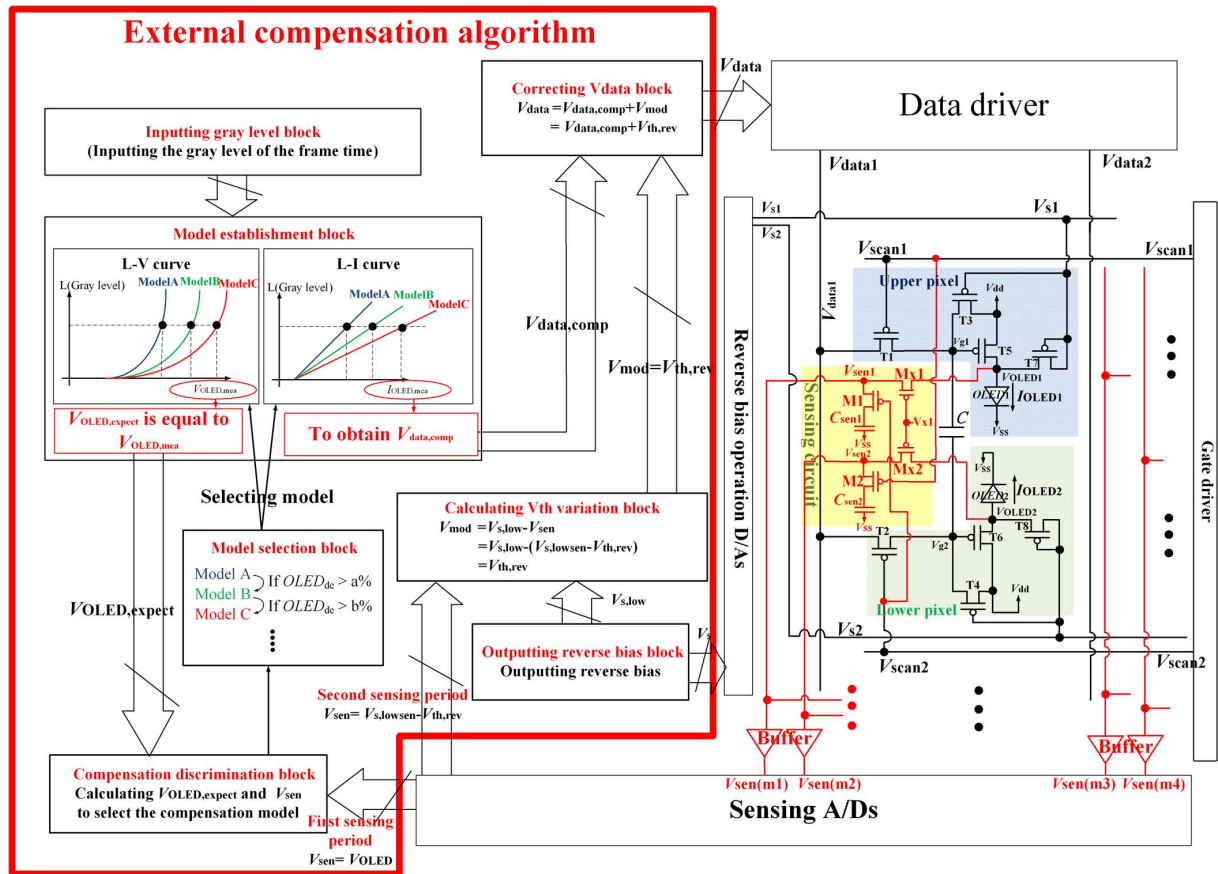


Fig. 1. An external compensation algorithm and the sensing circuit with the 4T0.5C pixel circuit.

To achieve better compensation precisions over a longer period of OLED compensations, in this study, a large-sized data bank of OLED's electro-optical models prescribing the relations between luminance and current ( $L - I$ ) and luminance and voltage ( $L - V$ ) of an OLED is established based on a large amount of prior, off-line measurements and indexed by a newly-defined degradation indicator. During operations, based on these models, a new external compensation algorithm applied to a sensing and 4T0.5C pixel drive circuit [9] is proposed herein to render accurate luminance of an AMOLED panel, even though OLED degradation is possibly aggravated by a number of compensations activated. Note that using the proposed method, OLEDs can be compensated to required luminance regardless of degradation status, but paying the price of hardware establishment to execute the compensation algorithm and to store large-scale  $L - I$  and  $L - V$  models. In addition to degradation compensation, the proposed algorithm with pixel circuit is capable of compensating threshold voltage ( $V_{th}$ ) variation of TFTs in pixels and applying reverse bias to alleviate OLED degradation. Note that  $V_{th}$  variation might lead to display non-uniformity. A number of past studies [16], [17] have worked on similar issues related to  $V_{th}$  variation. Special designs in pixel circuit and addressing timing procedure are presented to integrate successfully the functions of compensating aggravated degradation,  $V_{th}$  variation and reverse biases to alleviate OLED degradation.

The algorithm establishment is described in Section II. In Section III, the experiment is accomplished by the fabricated 4T0.5C pixel circuit operated with the sensing circuit and external algorithm to validate the performances of both compensating and alleviating OLED degradation, and  $V_{th}$  variation compensation. Finally, all study conclusions are summed in Section IV.

## II. THE ALGORITHM

The essence of the external compensation algorithm designed in this study is illustrated by Fig. 1, where the computations by the algorithm are shown in blocks in a red frame, while the rest is the pixel circuits. The algorithm performs jobs of (1) detecting OLED anode voltage to assess its degradation, (2) compensating OLED emission by re-calculating new  $V_{data}$ 's, (3) sensing  $V_{th}$  variations of TFTs and performing compensation, and (4) applying reverse biases to actively alleviate OLED degradation.

The blocks in the red frame in Fig. 1 include *compensation discrimination*, *model selection*, *model establishment*, *inputting gray level*, *outputting reverse bias*, *calculating  $V_{th}$  variation*, and *correcting  $V_{data}$* . The required computations in these blocks can be executed by a micro-processor. This processor accepts sensed inputs from the sensing circuit (in yellowish area) in the pixel and converted them to digits via analog-to-digital converters (A/Ds). Note that the sensing circuit detects OLED anode voltages in a given portion of a single-image addressing

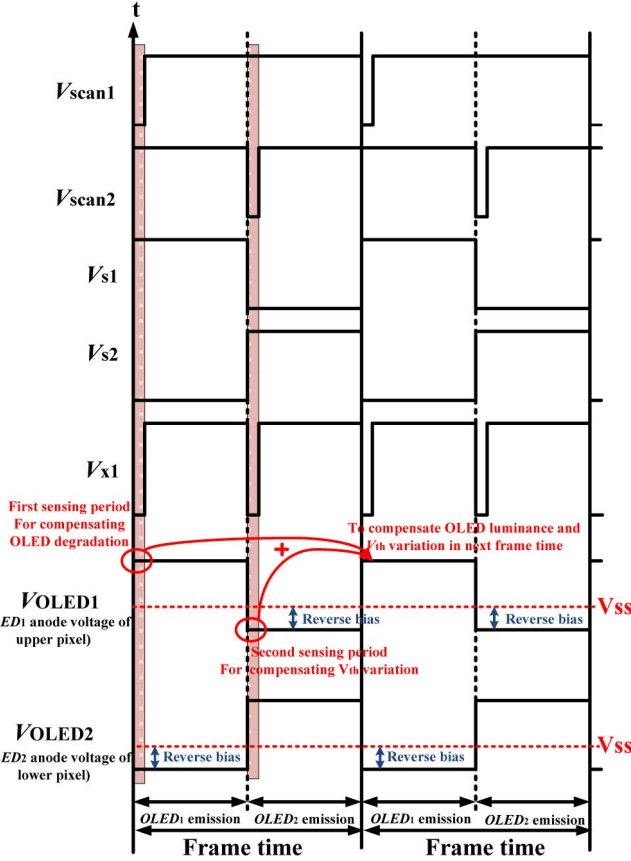


Fig. 2. Timing diagram for the 4T0.5C pixel circuit and sensing circuit.

frame, and then provides the algorithm an indication of OLED degradation level [3], [4]. Based on the sensed OLED anode voltage, the algorithm calculates the corrected  $V_{data}$ 's to output to the data driver for compensating the OLED degradation and  $V_{th}$  variation. The compensation operation is detailed in the following subsections.

### A. Operation of Pixel and Sensing Circuit

The pixel circuit at the right side of Fig. 1 illustrates a couple of 4T0.5C pixel circuits in light blue and green and also a sensing circuit in yellow. The 4T0.5C pixel circuits were presented in [9] while the sensing circuit is newly proposed in this study for sensing the OLED degradation level. The associated timing diagram of the pixel circuits is shown in Fig. 2, where two frames are considered to elaborate the compensation algorithm.  $V_{scan1}$  and  $V_{scan2}$  in both Figs. 1 and 2 represent the scan line signals for the first and second row, respectively.  $V_{s1}$  and  $V_{s2}$  are the OLED reverse biases applied in the non-emission periods to actively alleviate OLED degradation.  $V_{x1}$  is the control signal on switches  $M_{x1}$  and  $M_{x2}$  to activate/de-activate the sensing function of the designated pixel circuit.  $V_{OLED1}$  and  $V_{OLED2}$  denote the anode voltages of OLEDs in the upper and lower pixels, respectively, in Fig. 1. As the control signals in Fig. 2 are input into the pixel circuits in Fig. 1, a couple of 4T0.5C pixel circuits operate in a way that  $OLED_1$  emits while

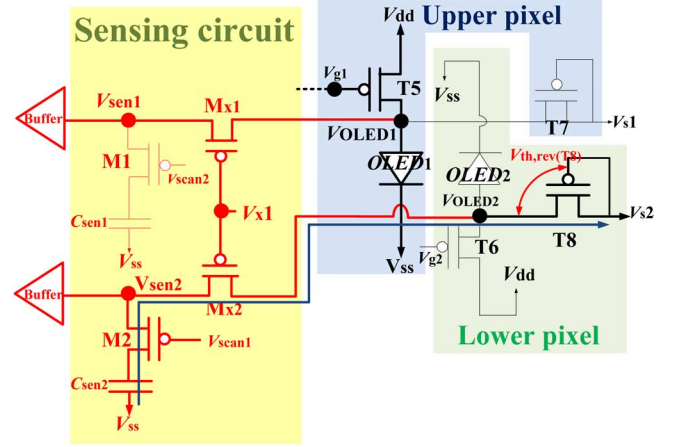


Fig. 3. Circuit operation for sensing in Fig. 1 during the first sensing period.

$OLED_2$  is in reverse bias period, and vice versa. According to the operation of pixel circuit in [9], this 4T0.5C pixel circuit owns both merits of alleviating OLED degradation by applying reverse bias in the first half of a frame time and maintaining high-resolution display by sharing a capacitor between two adjacent pixels. However, OLED degradation and  $V_{th}$  variation still need to be compensated by an external driving algorithm.

Based on the research works reported in [3], [4], one of the OLED degradation characteristics is that the anode voltage of OLED component inevitably increases for a long-time drive. This increased anode voltage of OLED is sensed in this study to serve as an indicator for a given degradation level of OLED [3], [4]. With mechanism of sensing degradation in hands, the operation on the sensing circuit is next distilled and the associated driving timing diagram is designed and illustrated by Fig. 2. In this figure, the anode voltages of two OLEDs,  $V_{OLED1}$  and  $V_{OLED2}$ , are sensed and used to determine the level of OLED degradation. To elaborate the sensing mechanism, the partial pixel circuit associated with  $OLED_1$  as shown in Fig. 3 is considered to describe the operation of sensing circuit during the first sensing period in Fig. 2. In this period, according to the operation of pixel circuit in [9],  $OLED_1$  in Fig. 3 emits, while  $OLED_2$  is in reverse bias period. Meanwhile, in the sensing circuit,  $V_{x1}$  and  $V_{scan2}$  are operated at the low and high level, respectively. The anode voltage of  $OLED_1$ ,  $V_{OLED1}$ , is sensed to a buffer as

$$V_{sen1} = V_{OLED1}. \quad (1)$$

On the other hand,  $V_{x1}$  and  $V_{scan1}$  are operated at the low level to charge  $C_{sen2}$  in order to sense the anode voltage of  $OLED_2$ ,  $V_{OLED2}$ . The procedure is utilized to acquire the  $V_{th}$  variation of  $T_8$ ,  $V_{th,rev}(T_8)$ , in the reverse bias period of  $OLED_2$  as shown in Fig. 2. The details of  $V_{th}$  compensation are described in subsequent Section II-G.

The sensing results,  $V_{sen1}$  and  $V_{sen2}$ , are then utilized in the following algorithm blocks to process the compensation procedures.

### B. Compensation Discrimination Block

In this block, the sensed anode voltage of  $OLED_1$ ,  $V_{sen1}$ , is utilized to serve as the degree of OLED degradation according to the equation defined by

$$OLED_{de} = \left( \frac{V_{sen} - V_{OLED,expect}}{V_{OLED,expect}} \right) \cdot 100\%, \quad (2)$$

which is in fact an error ratio of voltage compensation between the sensed voltage of OLED anode,  $V_{sen}$ , and the expected voltage of OLED anode,  $V_{OLED,expect}$ . This  $V_{OLED,expect}$  is obtained from a model established based on prior measurements in an off-line fashion. The compensation and prior measurement procedures are detailed in the subsequent Sections II-D and II-E, respectively. Via calculating (2), the degree of OLED degradation can be determined. The calculation results are input into the block of *Model Selection*, as shown in Fig. 1, in order to select an appropriate compensation model for maintaining the OLED luminance to expected levels.

### C. Model Selection Block

The computation associated with this block is to select the appropriate compensation model after successfully evaluating OLED degradation degree as stated in the *compensation discrimination* block. The models include the correspondences from luminance to current ( $L - I$ ) and from luminance to voltage ( $L - V$ ). For example, as shown in *Model selection* block in Fig. 1, a% and b% represent varied ratios of anode voltage error,  $OLED_{de}$ , in (2). As the anode voltage of degradation OLED increases, exceeding certain listed ratios, e. g. a% or b%, the selected model is changed from A to B or B to C, respectively, for compensating OLED emission. To build up the entire model bank, appropriate ranges of ratios,  $V_{OLED,expect}$ , are first determined to cover realistic operations of fabricated OLEDs. These ranges depend on required display brightness, different OLED devices/fabrications, the capability of data driver, and required capacity of model density for computation accuracy.

### D. Blocks of Model Establishment and Inputting Gray Level

The computation in *Model establishment* block in Fig. 1 intend to establish two associated model curves of  $L - I$  and  $L - V$ , where  $L$ ,  $I$ , and  $V$  are gray level, compensated driving current, and expected voltage of OLED anode, respectively. Note that the compensation on OLED degradation executed by this block is made possible with the required gray levels for a given image input from the *inputting gray level* block, also shown in Fig. 1. Based on the models of  $L - I$  and  $L - V$  provided and selected by blocks of *Model Establishment* and *Selection*, respectively, the desired OLED compensating current,  $I_{OLED,mea}$ , can be calculated. With this current, the proposed algorithm in the block of *Model Establishment* further calculates required input data-line voltage based on designed pixel circuit, which is achieved by solving the governing equation of the drive TFT for  $V_{data,comp}$ , i.e.,

$$I_{OLED,mea} = K(V_{data,comp} - V_{dd} - V_{th,drive})^2, \quad (3)$$

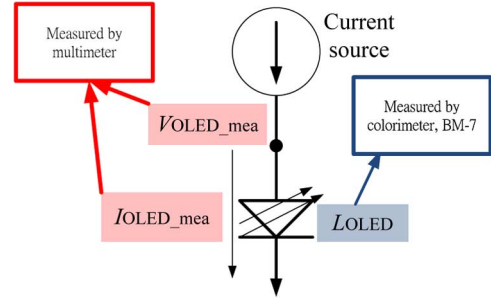


Fig. 4. Measurement for establishing OLED models.

where  $K$  incorporates mobility, gate capacitor  $C_{ox}$ , and the aspect ratio of driving TFT.  $V_{th,drive}$  is the threshold-voltage of the driving TFT.  $V_{data,comp}$  is the corresponding data-line voltage.  $V_{data,comp}$  calculated by (3) is obtained and output to the *correcting  $V_{data}$*  block as also shown in Fig. 1. Note that the block also accepts correction on  $V_{data}$  for  $V_{th}$  variation compensation. The related details are given in subsequent Section II-G. As shown in Fig. 1, the compensated results of OLED degradation and  $V_{th}$  variation,  $V_{data,comp}$  and  $V_{mod}$ , are finally summed to output the data-line voltage,  $V_{data}$ . It should be noted at this stage that the established  $L - V$  curves provides the expected voltage of OLED anode,  $V_{OLED,expect}$ , to evaluate OLED degradation degree again in each frame time. As shown in the  $L - V$  curve of Fig. 1, the required gray level of this frame time is also set by *inputting gray level* block, while  $L - V$  curve output corresponding  $V_{OLED,expect}$  to *compensation discrimination* block. Then,  $V_{sen}$  is sensed to calculate with the  $V_{OLED,expect}$  for discriminating degradation degree again. Therefore, the degradation compensation procedures can be processed in each frame time repeatedly for realizing the on-line sense in each pixel.

### E. Models Based on Prior Measurement

The aforementioned curves of  $L - I$  and  $L - V$  are established by prior off-line measurements.  $V_{OLED,expect}$  is set to be equal to measured OLED anode voltages,  $V_{OLED,mea}$ . The process to build a large-sized database of prior measurements for establishing curves of  $L - I$  and  $L - V$  are detailed in this subsection.

The setup for acquiring prior measurements includes a current source and an OLED component as shown in Fig. 4. In this figure,  $V_{OLED,mea}$  denotes the anode voltage of the OLED, while  $I_{OLED,mea}$  is the driving current generated from an assumed current source, which are all recorded by a multi-meter in the measurement process.  $L_{OLED}$  is the luminance emitted by the OLED, which is recorded by a colorimeter, BM-7. Two curves,  $L - I$  and  $L - V$ , are recorded for varied OLED drive currents. Resulted measurements are in fact used to affirm the relations among  $L_{OLED}$ ,  $V_{OLED,mea}$ , and  $I_{OLED,mea}$ . Note that as previously defined, the level of OLED degradation is evaluated and indicated by the anode voltage of OLED,  $V_{OLED,mea}$ . During measurement, the OLED is allowed to be driven for an extensive period of time for the presence of OLED degradation,

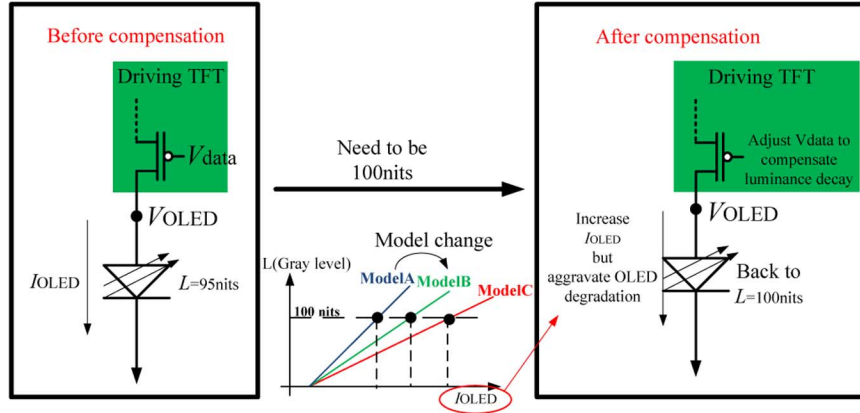


Fig. 5. Compensation on an OLED in a panel with degradation aggravation.

until the degradation level pre-defined in (2) reaches pre-designated values, say  $a\%$ ,  $b\%$ ,  $\dots$ , etc. Between these pre-designated ratios, local models of  $L-I$  and  $L-V$  can successfully be established, as denoted by Model A, B,  $\dots$ , etc, in blocks of *Model Establishment and Selection* in Fig. 1. In practice, the discrete measurement data for prescribing these local models are stored into the memory for use. In operations of an AMOLED display panel, as OLEDs degrade, the data driver selects the appropriate local model based on the sensed anode voltage of OLED, and then output the corrected data voltage for compensating OLED luminance decay. Fig. 5 illustrates aforementioned compensation process on an OLED.

It should be noted that as shown in Fig. 5, the OLED current,  $I_{OLED}$ , is increased in operation to compensation degradation for achieving required emitted luminance. This increased OLED current however aggravates degradation based on fundamental principles of OLEDs, in fact resulting in an extra increase in  $V_{OLED}$ . Fig. 6(a) illustrates the realistic evolution of  $V_{OLED}$  as the OLED is compensated for required luminance. In this figure, between X and Y or Z and U, local models A or B are employed, respectively, for predicting behaviors of the driven OLED. The corresponding instant at Y is when the OLED degradation indicator,  $OLED_{de}$ , exceeds prescribed  $a\%$  and compensation has to be executed. The compensation in fact increases the OLED current by the amount calculated by local model A in order to deal with degradation to achieve desired emitted luminance. The anode voltage of the OLED thus appears in a certain jump at the point Y when the OLED current is increased deliberately for compensation.

Fig. 6(b) illustrates the evolution of OLED anode voltage when establishing the model by a special method based on prior measurement, where  $V_{OLED,mea}$  represents the anode voltage of OLED in the measurement procedure of Fig. 4. The point W represents the moment of recording initial  $L-I$  and  $L-V$  curves of model A. After increasing  $a\%$  voltage as calculated in (2),  $L-I$  and  $L-V$  curve of model B are recorded at the moment of point V. The blue dashed line represents the prior measurement without adjusting current source for emulating the compensation state, where point R is the moment to record  $L-I$  and  $L-V$  curves of model C, obviously. However, according to the typical voltage history at OLED anode in Fig. 6(a), the anode voltage needs to be raised to maintain luminance just like the

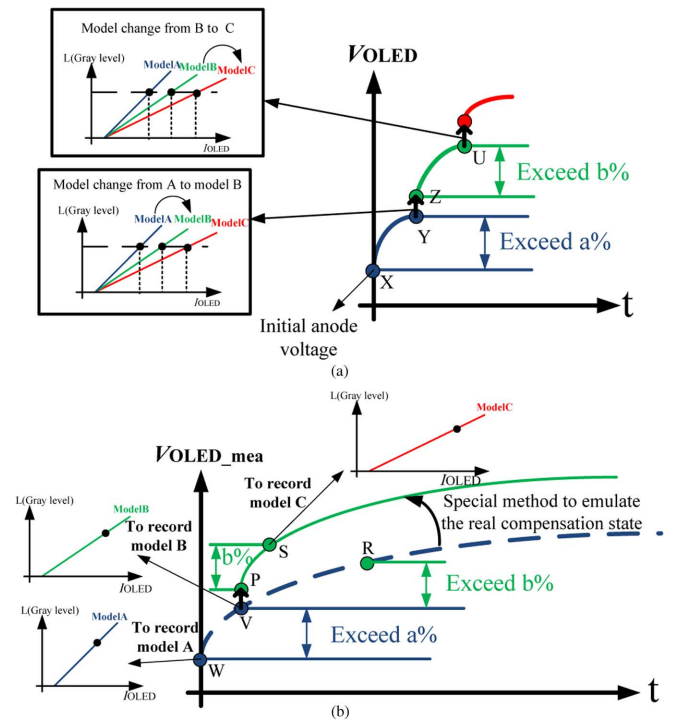


Fig. 6. (a) Typical voltage history at OLED anode during compensation. (b) Local model establishment based on measurement.

point Y is changed to point Z. Therefore, the degradation curve of prior measurement also needs to be changed to follow the green solid line, since the compensation procedures aggravate OLED degradation. Consequently, adjusting the current source of Fig. 4 after each prior model establishment for emulating typical anode voltage history is designed. For example, in Fig. 7, after recording model B at point V, the current of prior measurement in Fig. 4,  $I_{OLED,mea}$ , is increased to maintain 100 nits luminance emulating the compensation procedures in Fig. 5. The degradation curve of local model measurement after recording model B is hence corrected to be green solid line as shown in Fig. 6(b). When voltage error ratio increases exceeding  $b\%$ , model C is recorded at point S rather than point R, since the special method based on prior measurement emulate the aggravated OLED degradation. The local models are also recorded

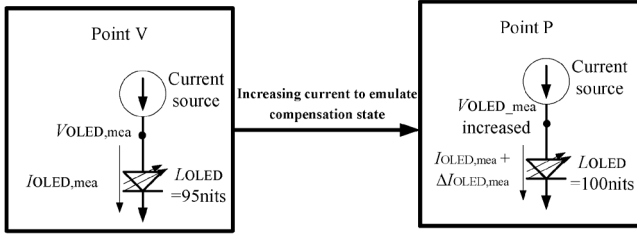


Fig. 7. Compensation activated with aggravated OLED degradation considered.

continually until they satisfy compensation requirements. Following this method, the required local models of external algorithm do not need to be established according to the various and complicated mathematical equations as using the diverse OLED devices. Even though the compensation state aggravates OLED degradation, this special method based on prior measurement can also achieve accurate compensation.

#### F. Outputting Reverse Bias Block

The *Outputting reverse bias* block as illustrated in Fig. 1 outputs the required reverse biases to the pixel circuit for alleviating OLED degradation. Appropriate levels of reverse are selected for satisfactory effects of easing OLED degradation [6]. This reverse bias is applied to one pixel as shown in Fig. 2 in the emission period of another pixel in each display frame time.

#### G. Blocks of Calculating $V_{th}$ Variation and Correcting $V_{data}$

During the sensing period in each display frame, as illustrated in Fig. 2, the  $V_{th}$  variation is sensed and compensated by subsequent related calculations. The associated works are in the block of *Calculating  $V_{th}$  variation* and *Correcting  $V_{data}$*  in Fig. 1. Since the operations of sensing  $V_{th}$  variations in upper or lower pixels are identical, the details of *Calculating  $V_{th}$  variation* is described herein only for  $OLED_2$  in the lower pixel.

As illustrated in Fig. 3, the switches of  $M_{x2}$  and  $M_2$  are controlled by  $V_{x1}$  and  $V_{scan1}$ , respectively. During the reverse bias period of  $OLED_2$  in Fig. 2,  $T_6$  is cut off, while the anode voltage of  $OLED_2$ ,  $V_{OLED2}$ , is at the reverse bias level by applied appropriate  $V_{s2}$ . Therefore, when charging  $C_{sen2}$  until the steady state,  $V_{OLED2}$  becomes

$$V_{OLED2} = V_{sen2} = V_{s2,low\text{sen}} - V_{th,rev}(T8), \quad (4)$$

where  $V_{s2,low\text{sen}}$  denotes the sensed low-voltage level of  $V_{s2}$ . This charging result is then input into the external compensation algorithm through a buffer and sensing analog-to-digital converters (A/Ds) as shown in Fig. 1. The block of *Calculating  $V_{th}$  variation* next calculates the sensed  $V_{sen2}$  to obtain required  $V_{th}$  variation information as

$$V_{mod} = V_{s2,low} - V_{sen2}, \quad (5)$$

where  $V_{s2,low}$  is obtained from the operations of the *Outputting reverse bias* block. Combination of (4) and (5) leads to

$$V_{mod} = V_{s2,low} - (V_{s2,low\text{sen}} - V_{th,rev}(T8)), \quad (6)$$

where  $V_{s2,low}$  is obviously equal to  $V_{s2,low\text{sen}}$ . Therefore,  $V_{mod2}$  can be derived by

$$V_{mod2} = V_{th,rev}(T8), \quad (7)$$

where  $V_{th,rev}(T8)$  represents the sensed threshold voltage of  $T8$ , as enabled by the operation in Fig. 3. The derived  $V_{mod}$  is next used to modify the OLED data-line voltage for  $V_{th}$  compensation by

$$\begin{aligned} V_{data} &= V_{data,comp} + V_{mod} \\ &= V_{data,comp} + V_{th,rev}, \end{aligned} \quad (8)$$

where  $V_{data}$  is the final data-line voltage with compensation on both OLED degradation and  $V_{th}$  variation. Note that the proposed degradation compensation process is detailed in Section II-D.  $V_{data}$  in (8) is output to data line and the resulted driving current for the designed pixel can be derived based on basic circuit theory as

$$\begin{aligned} I_{OLED} &= K(V_{data} - V_{dd} - V_{th,drive})^2 \\ &= K(V_{data,comp} + V_{th,rev} - V_{dd} - V_{th,drive})^2, \end{aligned} \quad (9)$$

where  $K$  consists of mobility, gate capacitor  $C_{ox}$ , and the aspect ratio of the driving TFT.  $V_{th,drive}$  is the threshold of the driving TFT. It is seen in (9) that if  $V_{th,rev}$  is close to  $V_{th,drive}$ , the  $V_{th}$  variation is canceled in the current equation. In this way, the OLED luminance degradation is compensated by  $V_{data,comp}$ , as evident in (9).

To explore the performance of compensating OLED degradation and  $V_{th}$  variation by the proposed design, the 4T0.5C pixel is fabricated to work with the proposed external compensation algorithm operated on a field programmable gate array (FPGA) module.

### III. EXPERIMENT VALIDATION

#### A. Model Establishment

The model establishment for use by the external algorithm is conducted following the operations illustrated by Figs. 4 and 7. The detailed steps are given in Section II-E. Note that since the anode voltage of OLED increases in a highly-nonlinear and unpredictable fashion, the error ratios defined in (2),  $OLED_{de}$ , are designated corresponding to 20% drops in OLED emitted luminance, which are 8.54% for model-switching between model A and model B, and 2.57% for model-switching between model B and model C, for a test 14-in AMOLED display in laboratory. Exemplary measurement results of local  $L - I$  and  $L - V$  curves are shown in Fig. 8(a) and (b). Using these curves, the external algorithm is able to output the appropriate  $I_{OLED}$  and  $V_{OLED,expect}$  for required gray levels (luminances), the process of which is included in Fig. 1. Note herein that the aforementioned designated 20% drops can be easily devised to smaller levels to establish finer local models of  $L - I$  and  $L - V$ . The related experimental results of compensation are presented in Section III-D.

#### B. Experimental Setup and Process

The experiment system is shown by a photograph in Fig. 9. The low-temperature poly silicon (LTPS) TFTs fabricated by

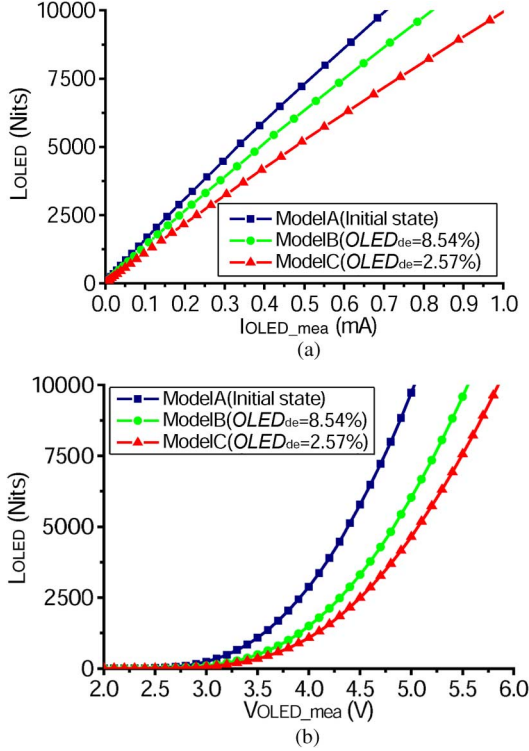


Fig. 8. Local models of (a)  $L - I$  and (b)  $L - V$  curves.

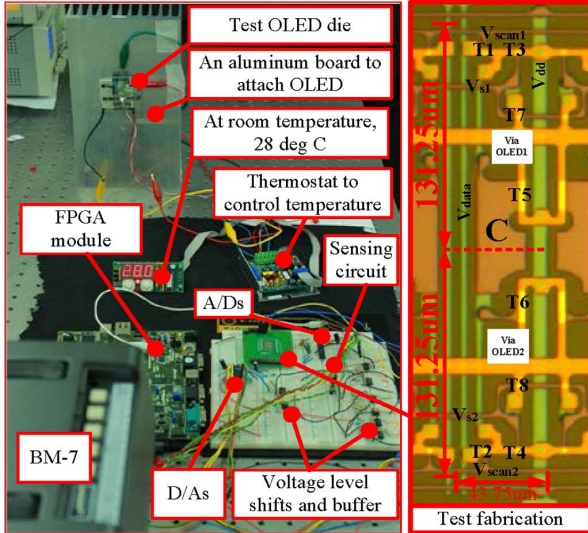


Fig. 9. Experiment system.

excimer laser annealing (ELA) are employed herein to fabricate the proposed 4T0.5C pixel [9]. To investigate the varied experimental performances including OLED degradation compensation and alleviation, and rule out the effects of temperature on OLED luminance, a system set with a drive circuit with adequate power for 100 pixels is orchestrated and wire-bonded to a single test OLED die in  $0.3 \times 0.3 \text{ cm}^2$ . The OLED die is attached at the bottom of an aluminum board in order to control at room temperature, 28 deg C, using a commercialized control unit and based on the feedback signals from a thermostat. A colorimeter BM-7 is utilized to measure the OLED luminance. Note that using a single OLED die for experiment herein could

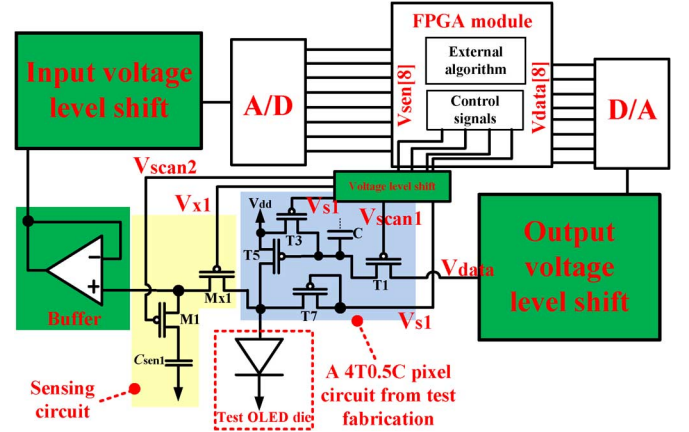


Fig. 10. Experiment setup for compensation by implementing the external compensation algorithm to a fabricated test panel.

obtain measurement data slightly different from a large-sized panel due to known IR-drop phenomenon [18]. However, the main focus of the current work is on the effectiveness of the proposed emission compensation algorithm, not the size effect of a panel.

The experiment process for compensation is illustrated in Fig. 10, where  $L - I$  and  $L - V$  curves are embedded into a FPGA module via forging a code in Verilog hardware description language (HDL). In this code, a frequency divider written by Verilog HDL is designed to output required 60 Hz signals,  $V_{scan1}$ ,  $V_{scan2}$ ,  $V_{s1}$ ,  $V_{s2}$ , and  $V_{x1}$ , from the clock generator in the FPGA module.  $V_{dd}$  and  $V_{ss}$  are set to be dc voltages of 6 V and  $-5$  V, respectively. The scan line signals,  $V_{scan1}$ ,  $V_{scan2}$ , and  $V_x$  all range from  $-5$  to 10 V, while enabling signals of reverse bias,  $V_{s1}$  and  $V_{s2}$ , are set from  $-10$  to 10 V according to the required reverse bias. Digital-to-analog converters (DACs) and analog-to-digital converters (ADCs) are used for signal transformations. Buffers and voltage level shifts are used to adjust voltage levels to conform to requirement of the FPGA module and pixel circuit.

### C. Compensating $V_{th}$ Variation

The experiment for validating  $V_{th}$  compensation is conducted by using two test pixel circuits, named A and B. Without compensation by the external algorithm, the luminance curves are measured, further normalized by maximums, and then shown in Fig. 11(a). It is seen from this figure that differences in OLED luminance is present with average of  $\pm 17.8\%$  between test pixels A and B.

On the other hand, Fig. 11(b) shows the experiment results with  $V_{th}$  compensation enabled. In this figure, lower difference in OLED emitted luminance is obtained with compensation. The difference is reduced from previous  $\pm 17.8\%$  to 3.2%. This reduction in emission difference validates well the expected performance of compensating  $V_{th}$  variation due to fabrication process.

### D. Compensating and Alleviating OLED Degradation

In addition to handle  $V_{th}$  variation, the main function of the proposed pixel circuit along with the external algorithm is to compensate and alleviate OLED degradation by established

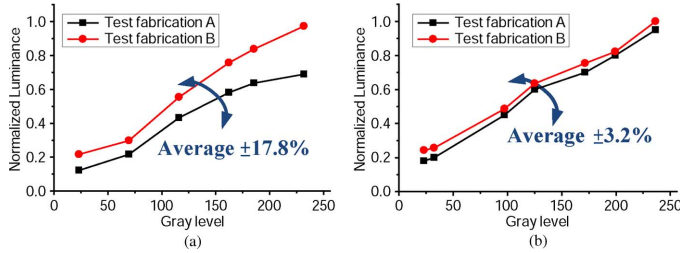


Fig. 11. Experiment results in luminance for varied gray levels; (a) without  $V_{th}$  compensation and (b) with compensation.

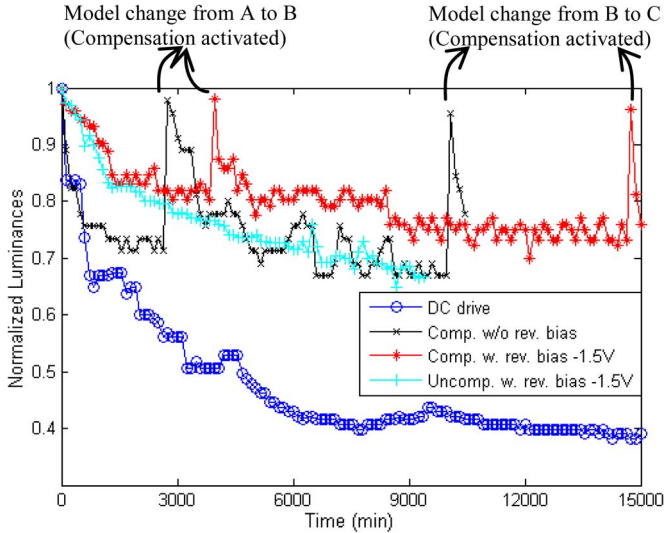


Fig. 12. Experiment results of compensating OLED degradation.

local models and reverse biases, respectively. Experimental results are summarized and shown in Fig. 12. The data are collected for an extensive period of time. Four cases of data with are presented in this figure. One presents the data for an OLED biased by a DC drive. Since the storage capacitance in a typical 2T1C circuit is often designed to be charged to steady state in a very short period of time as compared to the whole frame time, the OLED component in the 2T1C pixel circuit can be regarded in emitting status in the full frame time. Therefore, the wire-bonded DC drive in Fig. 12 can be regarded almost equivalent to the drive by 2T1C pixel circuit. The other two apply the compensation methods proposed with two different biases of 0 and  $-1.5$  V, i.e., without and with reverse biases enabled in the half current-off period illustrated by Fig. 2 in a addressing frame of an OLED panel. The last one presents un-compensated luminances but with reverse  $-1.5$  V for comparison.

It is seen from Fig. 12 that the proposed OLED degradation compensation is automatically activated twice for each of the two cases with 0 and  $-1.5$  V as reverse biases. At the four instants of compensation activated, the OLED emitted luminances are elevated back to original-required normalized luminance of one, showing the very effectiveness of the proposed pixel circuit, the external compensation algorithm and local models of  $L - I$  and  $L - V$  established. Note that the 20% degradation during operation is due to the fact that the OLEDs continue to

degrade between the employments of different OLED models. This 20% is actually set by the designer based on the mechanism proposed in this study. It can be set much smaller (like 5% or even any given smaller value), with a larger set of  $L - V$ ,  $L - I$  OLED models to be established and more frequent employments of new, different models during operations. Furthermore, the luminance curve with DC drive representing 2T1C circuit shows serious luminance decays as compared to other two cases with compensation, indicating the necessity of applying the compensation proposed. It is also shown in this figure that the luminance decay of the curve with reverse bias applied (red) is slower than the one (black) without reverse bias, demonstrating well the favorable performance of proposed method of reverse bias. Finally, another curve shown in this figure contains uncompensated OLED luminances with reverse bias  $-1.5$  V, which are shown clearly lower than the compensated curve after the first compensation for an extensive period of time, even with the accelerated drops right after the compensations applied each time. This demonstrates well the improvements offered by the proposed compensation method not only in emitting correct luminance right at compensations but also leading to smaller luminance errors afterward based on corrected, new models. Note that accelerated, exponential-like drops are always present upon a sudden increase in OLED current which complies with the basic emission microelectronic physics of OLEDs [19].

#### IV. SUMMARY

An external OLED compensation algorithm along with a pixel sensing/addressing circuit is designed successfully. The algorithm is capable of offering the applied voltage to achieve a given emitted luminance with consideration of OLED degradation. This is made possible by establishing two groups of data-base models for predicting relations between emitted luminance and voltage/current of the OLED based on a large amount of off-line measurements. Methods of model measurements are designed to emulate possible aggravated degradation of OLED for the more accurate compensation. The models are further extended to those for the cases as OLED degradation amounts to higher levels. On the other hand, the designed pixel circuit provides a chance to estimate the OLED degradation level in an on-line fashion by sensing OLED voltage within a selected short time span in a typical image frame time. With sensed OLED voltages, one is able to choose the correct data-based models of luminance-current to perform compensation. A test pixel is fabricated and driven with the sensing circuit and established compensation algorithm. Experimental results show that the compensation is effective in the evidence of displaying desired OLED luminance. Moreover,  $V_{th}$  variation is also shown compensated effectively and the applied reverse bias is able to alleviate OLED degradation.

#### ACKNOWLEDGMENT

The authors would like to thank AU Optronics Corporation, Hsinchu, Taiwan, for their assistance in fabricating the OLED pixel circuit for testing and appreciate the support from National Chip Implementation Center.



## REFERENCES

- [1] C. Hosokawa, M. Matsuura, M. Eida, K. Fukuoka, H. Tokailin, and T. Kusumoto, "Full-color organic EL display," *J. SID*, vol. 6, no. 4, pp. 257–260, 1998.
- [2] D. Y. Kondakov, J. R. Sandifer, C. W. Tang, and R. H. Young, "Nonradiative recombination centers and electrical aging of organic light-emitting diodes: Direct connection between accumulation of trapped charge and luminance loss," *J. Appl. Phys.*, vol. 93, no. 2, pp. 1108–1119, Jan. 2003.
- [3] J. Shen, D. Wang, E. Langlois, W. A. Borrow, P. J. Green, C. W. Tang, and J. Shi, "Degradation mechanisms in organic light emitting diodes," *Synth. Metals*, vol. 111, pp. 233–236, 2000.
- [4] M. Hack, J. J. Brown, J. K. Mahon, R. C. Kwong, and R. Hewitt, "Performance of high-efficiency AMOLED displays," *J. SID*, vol. 9, no. 3, pp. 191–194, 2001.
- [5] S. T. Lee, Z. Q. Gao, and L. S. Hung, "Metal diffusion from electrodes in organic light-emitting diodes," *Appl. Phys. Lett.*, vol. 75, no. 10, pp. 1404–1406, Sep. 1999.
- [6] M. Yahiro, D. Zou, and T. Tsutsui, "Recoverable degradation phenomena of quantum efficiency in organic EL devices," *Synthet. Metals*, vol. 111, pp. 245–247, Jun. 2000.
- [7] Y. J. Si, L. Q. Lang, Y. Zhao, X. F. Chen, and S. Y. Liu, "Improvement of pixel electrode circuit for active-matrix OLED by application of reversed-biased voltage," *IEEE Trans. Circuits Syst. II, Exp. Briefs*, vol. 52, no. 12, pp. 856–859, Dec. 2005.
- [8] K. Y. Lee and C. P. Chao, "A new AMOLED pixel circuit with pulsed drive and reverse bias to alleviate OLED degradation," *IEEE Trans. Electron Devices*, vol. 59, no. 4, pp. 1123–1130, Apr. 2012.
- [9] K. Y. Lee, Y. P. Hsu, and C. P. Chao, "A new 4T0.5C AMOLED pixel circuit with reverse bias to alleviate OLED degradation," *IEEE Electron Device Lett.*, vol. 33, no. 7, pp. 1026–1024, Jul. 2012.
- [10] G. R. Chaji, C. Ng, A. Nathan, A. Werner, J. Birnstock, O. Schneider, and J. Blochwitz-Nimoth, "Electrical compensation of OLED luminance degradation," *IEEE Electron Device Lett.*, vol. 28, no. 12, pp. 1108–1110, Dec. 2007.
- [11] T. Kohno, H. Kageyama, M. Miyamoto, M. Ishii, N. Kasai, N. Nakamura, and H. Akimoto, "High-speed programming architecture and image-sticking cancellation technology for high-resolution low-voltage AMOLEDs," *IEEE Trans. Electron Devices*, vol. 58, no. 10, pp. 3444–3452, Oct. 2011.
- [12] C. L. Lin and Y. C. Chen, "A novel LTPS-TFT pixel circuit compensating for TFT threshold-voltage shift, OLED degradation for AMOLED," *IEEE Electron Device Lett.*, vol. 28, no. 2, pp. 129–131, Feb. 2007.
- [13] H. J. In and O. K. Kwon, "External compensation of nonuniform electrical characteristics of thin-film transistors and degradation of OLED devices in AMOLED displays," *IEEE Electron Device Lett.*, vol. 30, no. 4, pp. 377–379, Apr. 2009.
- [14] H. J. In, K. H. Oh, I. Lee, D. H. Ryu, S. M. Choi, K. N. Kim, H. D. Kim, and O. K. Kwon, "An advanced external compensation system for active matrix organic light-emitting diode displays with poly-Si thin-film transistor backplane," *IEEE Trans. Electron Devices*, vol. 57, no. 11, pp. 3012–3019, Nov. 2010.
- [15] U.-G. Min, H.-J. In, and O.-K. Kwon, "A real time video data adjusting method for active matrix organic light emitting diode displays with high image quality," *IEEE Trans. Consumer Electron.*, vol. 55, no. 4, pp. 2372–2376, Nov. 2009.
- [16] S. H. Jung, W. J. Nam, and M. K. Han, "A new voltage-modulated AMOLED pixel design compensating for threshold voltage variation in poly-Si TFTs," *IEEE Electron Device Lett.*, vol. 25, no. 10, pp. 690–692, Oct. 2004.
- [17] J. H. Lee, W. J. Nam, S. H. Jung, and M. K. Han, "A new current scaling pixel circuit for AMOLED," *IEEE Electron Device Lett.*, vol. 25, no. 5, pp. 280–282, May 2004.
- [18] M. H. Jung and O. Kim, "Voltage distribution of power source in large AMOLED displays," *J. Kor. Phys. Soc.*, vol. 48, pp. S5–S9, Jan. 2006.
- [19] B. M. Weon, S. Y. Kim, J.-L. Lee, and J. H. Je, "Evolution of luminance by voltage in organic light-emitting diodes," *Appl. Phys. Lett.*, vol. 88, 2006, Art. ID 013503.



**Kuei-Yu Lee** received the B.S. degree in electrical engineering from the National Taiwan Ocean University, Keelung, Taiwan, in 2007, and the M.S. and Ph.D. degrees in electrical control engineering from National Chiao Tung University, Hsinchu, Taiwan, in 2009 and 2012, respectively. His research interests focus on thin-film transistors and active-matrix organic light-emitting diode (OLED) display.

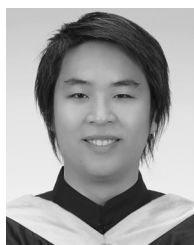


**Yen-Ping Hsu** received the B.S. degree from National Chiao Tung University, Hsinchu, Taiwan, in 2009, and the M.S. degree in electrical control engineering from National Chiao Tung University, Hsinchu, Taiwan, in 2011. His research interests focus on active-matrix organic light-emitting diode (OLED) display.



**Paul C.-P. Chao** (M'07) received the B.S. degree from National Cheng-Kung University, Tainan, Taiwan, in 1989, and the M.S. and Ph.D. degrees from Michigan State University, USA, in 1993 and 1997, respectively. He worked for the CAE department of Chrysler Corp in Auburn Hill, Detroit, MI, USA, for two years. He is currently a faculty member of the electrical engineering department at National Chiao Tung University (NCTU), Taiwan. In recent years, his research interests focus on interface analog circuit design for optical devices/systems, micro-sensors and actuators.

Prof. Chao was the recipient of the 1999 Arch T. Colwell Merit Best Paper Award from Society of Automotive Engineering, Detroit, USA; the 2004 Long-Wen Tsai Best Paper Award from National Society of Machine Theory and Mechanism, Taiwan; the 2005 Best Paper Award from National Society of Engineers, Taiwan; and the 2002/2003/2004 CYCU Innovative Research Award; 2006 the AUO Award; 2007 the Acer Long-Term 2nd-prize Award; The 2007/2008/2009 NCTU EEC Outstanding Research Award; the 2009 Best Paper Award from the Symposium on Nano-Device Technology; the 2010 Best Paper Award from the 20th Annual IEEE/ASME Conference on Information Storage and Processing Systems (ISPS). He was the Associate Provost of NCTU, the Secretary of IEEE Taipei Section, 2009–2010, and currently the founding chair of local chapter for the IEEE Sensor Council and an AdCom member of the IEEE Sensors Council. He is also the Associate Editors of three well-known SCI-index journals, *IEEE SENSORS JOURNAL*, *ASME Journal of Vibration and Acoustics* and *Journal of Circuits, Systems and Computers*. He is an ASME fellow.



**Wei-Dar Chen** received the B.S. degree in 2003 from Hsiuping University of Science and Technology, Taichung, Taiwan, in 2009, and the M.S. degree in electrical engineering from I-Shou University, Kaohsiung, Taiwan, in 2005. Currently, he is working towards the Ph.D. degree in electrical control engineering from National Chiao Tung University, Hsinchu, Taiwan. His research interests focus on photovoltaic control system and battery charging system.